

Analysis and Simulation of Strong Motion Records from Different Sites and Structure Based on HHT



Chen Qingjun, Yang Yongsheng

State Key Laboratory for Disaster Reduction in Civil Engineering, Tongji University, Shanghai, 200092, China

SUMMARY:

The time-frequency characteristics of the strong motion records and the dynamic response properties for a frame structure are studied by using Hilbert-Huang Transform(HHT). Meanwhile, the corresponding soil-structure interaction(SSI) system is simulated in this paper. Selecting the strong motion records of western U.S. in 1994 Northridge earthquake, the time-frequency characteristics of strong motion records on different sites(deep soft soil site, bedrock site and structural site) are analyzed respectively. By analyzing these results, the seismic response characteristics of deep deposit soil layers and SSI influence for the structure are discussed. Then selecting a 7-story RC frame structure(station code:24386) and the corresponding site as the case, the finite element model of SSI system is created and analyzed by the ANSYS program under the excitation of bedrock strong motion records. By comparing the calculated responses with the recorded data, the reasonableness of numerical model is verified and the factors that affect the model accuracy are discussed. the conclusions would provide useful reference for further work on this subject.

Keywords: HHT, Different types of sites, Soil-structure interaction, Numerical simulation, Strong motion record analysis

1. INTRODUCTION

The earthquake response observation is a primary mean of people studying the structural response and damage process under earthquake excitation, examining the existing seismic design theories and methods of structures. It is equivalent to the prototype tests that Engineering structures experienced earthquakes and obtained seismic response records, the shaking table model test is difficult to simulate the behaviours of structure in earthquake. Therefore, carrying out seismic research by strong earthquake record has been paid enough attention. For a long time, The methods of processing seismic records most commonly used in earthquake engineering field are the Fourier transform and Wavelet analysis. But these two methods are fundamentally based on stationary signals, when processing non-stationary signals like seismic records may cause some serious problems, such as energy leaks. HHT(Hilbert-Huang transform) method, presented by Huang of America NASA in 1998, is well suited for processing non-stationary signals and considered as a major breakthrough and transformation in the field of signal processing. Since HHT method was proposed, it quickly has been applied in various fields, such as earthquake data analysis, structure health diagnosis, damage identification, damage detection and system identification, and have achieved good results.

Soil-structure interaction(SSI), one of the most major subjects in the domain of earthquake engineering, has been paid comprehensive attention by international in recent decades. For the structures on the deep soft soil sites, natural period will be extended because of SSI. Since deep soft soil has amplification effect to low-frequency components of seismic waves, the dynamic response of structures supported on soft soil is bigger than the same structures supported on rigid sites. Particular, when the nature frequency of structure close to the predominant frequency of seismic wave, the structure will suffer more serious damage under earthquake. SSI studies have achieve rapid progress in recent decades and many researchers have done a great deal of works of linear SSI. But the studies of

nonlinear SSI are relative less, so it is necessary to do further research.

Selecting the strong motion records of western U.S. in 1994 Northridge earthquake, the time-frequency characteristics of records on different sites(deep soft soil site, bedrock site and structural site) are analyzed respectively by HHT method in this paper. By analyzing these results, the seismic response characteristics of deep deposit soil layers and the SSI effect to structure seismic response are discussed. Then a 7-story RC frame structure is selected as the case, the finite element model of SSI system is created and analyzed under the excitation of bedrock acceleration records by the ANSYS program. Then comparing the calculated results with the recorded data, the factors that affect the model accuracy in numerical simulation of SSI system seismic response are discussed.

2. ANALYSIS METHODS AND THE BASIC THEORY

2.1. HHT Method Introduction

The core idea of HHT method is that time series are decomposed into several IMF (Intrinsic Mode Functions) by EMD(Empirical Mode Decomposition), and then use Hilbert transform to compose analytic signals, obtain instantaneous frequency and Hilbert spectrum of the original data.

The idea of EMD is to define the “instantaneous equilibrium position” of original time series $x(t)$ by the average of upper and lower envelopes, and then extract the IMF. First, find out the local maximum and minimum values and connect the local maximum and minimum values respectively with cubic splines interpolation, get maximum envelope $x_{\max}(t)$ and minimum envelope $x_{\min}(t)$. Second, average $x_{\max}(t)$ and $x_{\min}(t)$, obtain instantaneous average $m(t)=[x_{\max}(t)+x_{\min}(t)]/2$. Finally, the original series $x(t)$ subtract the instantaneous average $m(t)$, obtain a new series $h(t)$ without low frequency components: $h(t)=x(t)-m(t)$. Check whether $h(t)$ satisfies the following two conditions of the IMF: (1)The number of peak points equal to the times of curve passing through 0 or a maximum difference of 1; (2) At any point, the average of the maximum envelope and minimum envelope equal to 0; If $h(t)$ satisfy the above two conditions, then $h(t)$ as a IMF denoted by $C_1(t)$; Else, $h(t)$ as the original series and repeat the above steps until it satisfies the conditions (1) and(2), then separate $C_1(t)$ from the original series: $x(t)-C_1(t)=R_1(t)$. Since the remainder $R_1(t)$ still contains longer period components, so $R_1(t)$ processed by repeating above steps as a new time series. After such process, the original series $x(t)$ is decomposed into n IMF and a residue $R_n(t)$:

$$x(t) = \sum_{i=1}^n C_i(t) + R_n(t) \quad (2.1.1)$$

The above process is EMD, the residual $R_n(t)$ represents the trend of original time series. IMF is very suitable for Hilbert transform in characteristics, then compose analytic signals and obtain instantaneous frequency. In brief, the Hilbert transform is the convolution of signal and $1/t$, so it's characterized by emphasis on local properties. The Hilbert transform of $C(t)$ given by:

$$\hat{C}(t) = \frac{1}{\pi} PV \int_{-\infty}^{+\infty} \frac{C(\tau)}{t-\tau} d\tau \quad (2.1.2)$$

Where PV represents the Cauchy principal value, analytic signal of $C(t)$ is defined by:

$$z(t) = C(t) + i\hat{C}(t) = a(t)e^{i\theta(t)} \quad (2.1.3)$$

where:

$$a(t) = [C^2(t) + \hat{C}^2(t)]^{1/2} \quad (2.1.4)$$

$$\theta(t) = \tan^{-1}[\hat{C}(t) / C(t)] \quad (2.1.5)$$

Eqn. 2.1.3 to Eqn. 2.1.5 are expressions in the polar coordinate system, $a(t)$ and $\theta(t)$ express instantaneous amplitude and phase clearly, which reflect the instantaneous characteristics of the IMF, the instantaneous frequency defined by:

$$\omega(t) = d\theta(t) / dt \quad (2.1.6)$$

After Hilbert transform, the amplitude and frequency are functions of time. The three dimension time-frequency spectrum $H(\omega, t)$ of original signal $x(t)$ can be got by displaying amplitude of all IMF on the frequency-time plane. Marginal spectrum $h(\omega)$ can be defined as follows:

$$h(\omega) = \int_0^T H(\omega, t) dt \quad (2.1.7)$$

Marginal spectrum represents the accumulated amplitude of each frequency point throughout the whole time. In addition, Instantaneous energy spectrum can be defined by

$$IE(t) = \int_{\omega} H^2(\omega, t) d\omega \quad (2.1.8)$$

The instantaneous energy spectrum represents signal energy changing with time. The Hilbert energy spectrum can be defined as follows:

$$ES(\omega) = \int_0^T H^2(\omega, t) dt \quad (2.1.9)$$

Hilbert energy spectrum represents the total energy of each frequency point, which express the accumulated energy throughout the whole time.

The innovation of HHT method are that the EMD is adaptive and without fixed priori base, different time series have different IMF. Instantaneous frequency expresses the local characteristics of signal, which do not need the entire wave to define the local frequency. It is a breakthrough compared with traditional methods which defined the harmonic signals as the base.

2.2. Numerical Methods and Soil Constitutive Models

Soil is strong nonlinear materials, and usually soften with increasing strain due to its nonlinear behavior. The equivalent linearization method is one of the primary method to estimate nonlinear characteristics of the sites under seismic excitation, this method considers nonlinear characteristics of soil by linear iterative calculation indirectly.

One-dimensional equivalent linearization method is based on two assumptions as follows: (1)The surfaces of bedrock and soil layers are horizontally and infinite extension in the horizontal direction. (2)The seismic wave is shear wave propagating from the bedrock to ground surface though soil layers. Seed and Idriss calculated the seismic response of horizontal site with equivalent linearization method first time in 1969. Since then, equivalent linearization method has been widely used in engineering field. Martin and Seed calculated the nonlinear seismic response of six one-dimensional sites with true nonlinear method and equivalent linearization method respectively, studies show that the results with equivalent linearization method and true nonlinear method are almost the same. Hadjian debugged some programs using earthquake records of Lotung nuclear power plant model, the studies show that the equivalent linearization method is feasible to calculate the seismic response of soil site.

For the studies of equivalent linear model, some scholar have proposed dynamic constitutive models for different types of soils, such as Seed-Idriss model, Sun-Colesorkhi model, Vucetic-Dobry model and Ishibashi-Zhang model etc. For the relationship between shear modulus and shear strain, this paper selects Seed-Idriss model for sand and Seed-Sun model for clay. For the relationship between damping ratio and shear strain, adopt Idriss model for both sand and clay in this paper. The value of selected models are shown in Tab. 2.1, and Fig. 2.1 is the corresponding figure. The bedrock under soil adopts the linear assumption that shear modulus and damping ratio are constants. The stiffness of structures and piles is much bigger than the soil stiffness, so elastic constitutive model is selected to simulate the structures and piles.

Table 2.1. Equivalent models of shearing modulus and damping ratio used in analysis

	γ (%)	0.0001	0.0003	0.001	0.003	0.01	0.03	0.1	0.3	1	3	10
Sand	G/G_{max}	1	0.99	0.96	0.9	0.76	0.57	0.3	0.15	0.06	0.04	0.03
	D (%)	0.48	0.8	1.5	3.2	5.7	9.5	15.2	20.5	24.6	27	28.5
Clay	G/G_{max}	1	1	1	0.981	0.941	0.847	0.656	0.438	0.238	0.144	0.110
	D (%)	0.48	0.8	1.5	3.2	5.7	9.5	15.2	20.5	24.6	27	28.5

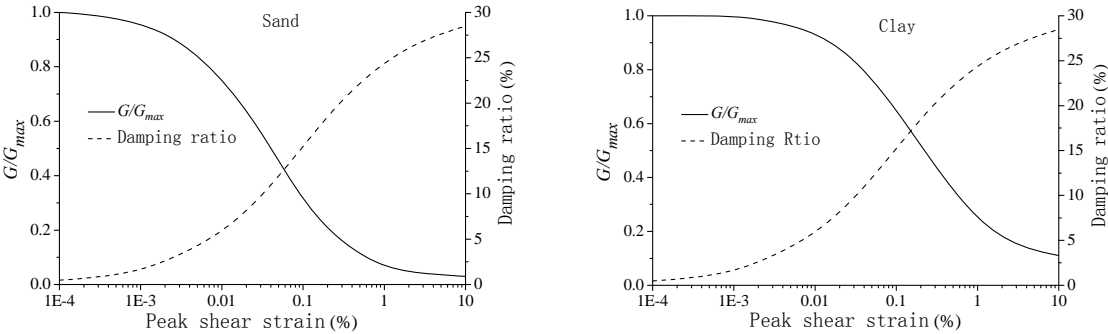


Figure 2.1. Equivalent models of shearing modulus and damping ratio for soil

3. SPECTRAL CHARACTERISTICS ANALYSIS OF STRONG MOTION RECORDS

Strong motion records on different sits(deep soft soil site, bedrock site and structure site) of western U.S. in 1994 Northridge earthquake are studied. The structure sites selected in this paper is a 7-story RC hotel building, it is located in the city of Van Nuys of the Los Angeles metropolitan area(at 34.221°N and 118.471°W, in central San Fernando Valley, N-W from downtown Los Angeles). This building was designed in 1965, constructed in 1966 and heavily damaged in 1994 Northridge earthquake. Due to the building's instrumentation, most acceleration response data of earthquakes has been collected, and many researchers have studied this building. Fig. 3.1 illustrates the location and orientation of the sixteen sensors. Fig. 3.2 shows the selected acceleration time histories and peak values of the acceleration response of structure are given in Tab. 3.1.

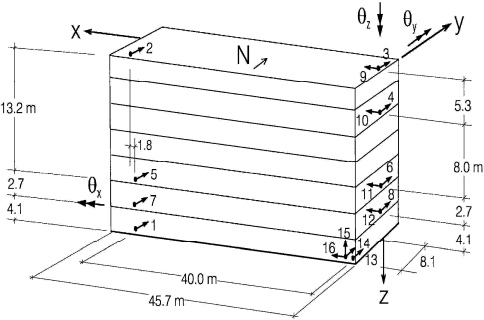
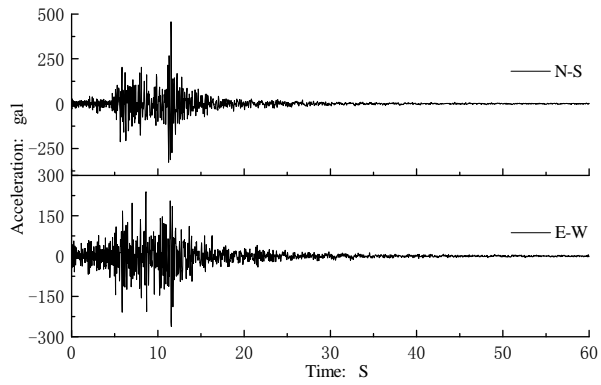


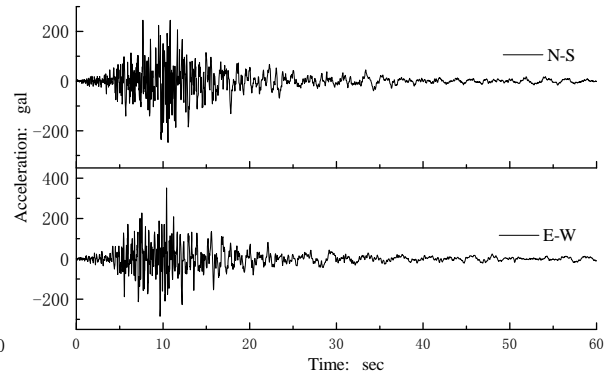
Figure 3.1. Locations of the sensors for channels 1-16

Table 3.1. Peak acceleration of channels 1-16

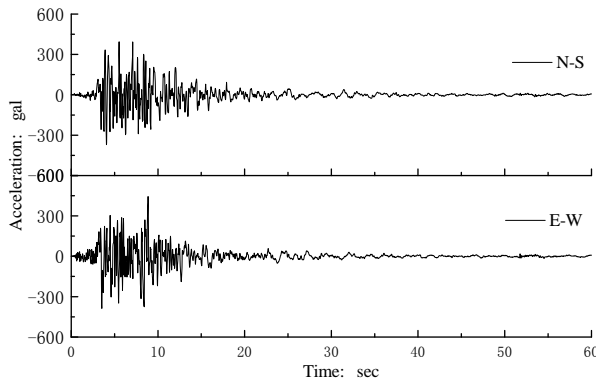
Channel	Peak(cm/sec ²)	Channel	Peak(cm/sec ²)
CH1	379.167	CH9	567.011
CH2	545.409	CH10	448.131
CH3	561.445	CH11	354.634
CH4	328.060	CH12	326.151
CH5	401.639	CH13	408.866
CH6	439.748	CH14	393.837
CH7	369.045	CH15	265.103
CH8	392.857	CH16	444.536



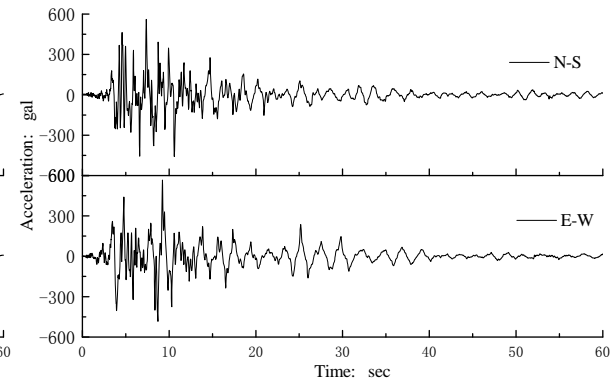
(a) Acceleration of bedrock motion



(b) Acceleration of ground motion



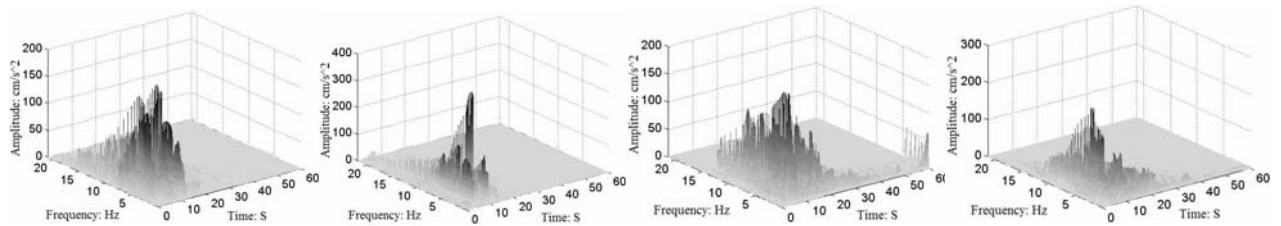
(c) Acceleration of foundation motion



(d) Acceleration of roof motion

Figure 3.2. Seismic acceleration time history curves

The time-frequency characteristics of the selected acceleration data are analyzed by HHT method. Fig. 3.3 to Fig. 3.6 present the three dimension time-frequency spectrum, and the marginal spectrum as shown in Fig. 3.7 to Fig. 3.9.



(a) E-W direction

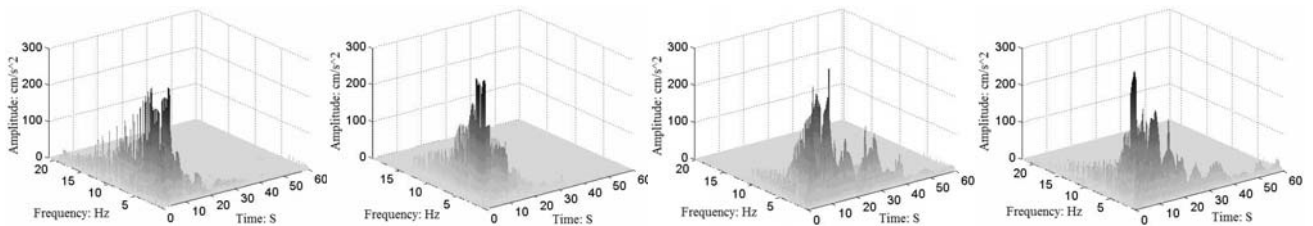
(b) N-S direction

Figure 3.3. Three dimension time-frequency spectrum of bedrock motion

(a) E-W direction

(b) N-S direction

Figure 3.4. Three dimension time-frequency spectrum of ground motion



(a) E-W direction

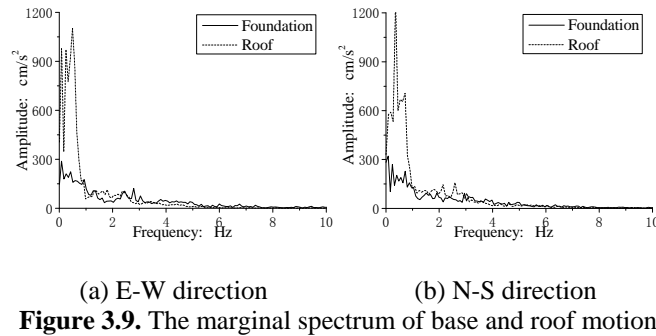
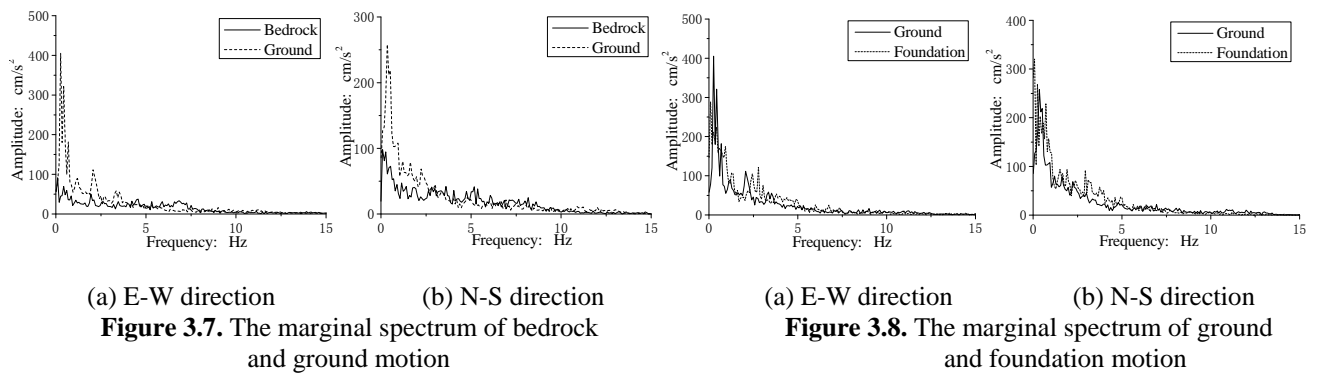
(b) N-S direction

Figure 3.5. Three dimension time-frequency spectrum of foundation motion

(a) E-W direction

(b) N-S direction

Figure 3.6. Three dimension time-frequency spectrum of roof motion



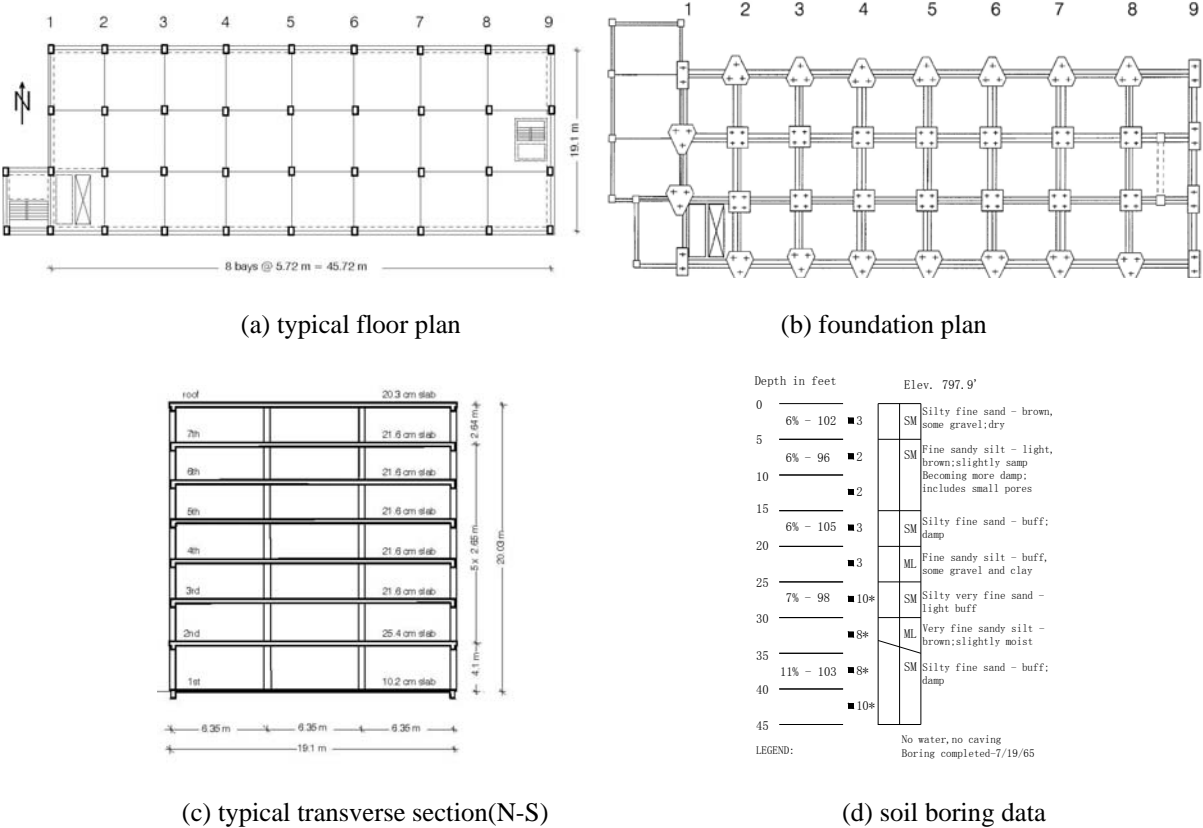
It can be shown from Fig. 3.3 to Fig. 3.6, the energy of bedrock motion is mainly concentrated between 0 to 15 second, the amplitude is almost close to 0 after 15 second; meanwhile, the energy of ground motion is mainly distributed between 0 to 30 second, the amplitude achieve maximum at 10 second and then gradually decay. The energy distribution of the structural foundation motion is very similar to the ground motion, but the SSI result in a rapid attenuation after 10 second and the value almost close to 0 after 20 second. The energy of structural roof motion has a wide distribution in time domain and shows a character of multi-peak distribution. The maximum amplitude appears in 10 second and with a tendency of slow attenuation.

From the comparison among acceleration marginal spectrums of bedrock motion, ground motion, structural foundation motion and roof motion, the following results can be gotten: deep soft soil has significant filtering effect for frequency characteristics of seismic waves, the low frequency components of ground motion is amplified and the high frequency component is reduced, the predominant period move towards to long-period. The SSI effect has slightly influence to the spectrum characteristics of seismic waves in this case. The marginal spectrum distributions of structural foundation motion and roof motion are quite different, and the maximum amplitude of the latter is about 4 times of the former. The acceleration of roof motion has considerable amplification.

4. NUMERICAL SIMULATION OF SSI NONLINEAR SEISMIC RESPONSE

Van Nuys Hotel is 19.1×45.72 m in plan(Fig. 4.1a), the typical framing consists of columns spaced at 6.35 m centers in the transverse direction and 5.72 m centers in the longitudinal direction. Spandrel beams surround the perimeter of the structure. Lateral forces in each direction are resisted by interior column-slab frames and exterior column spandrel beam frames. The added stiffness in the exterior frames associated with the spandrel beams creates exterior frames that are roughly twice as stiff as interior frames. The typical exterior columns are 35.56×50.8 cm oriented with the weak axis perpendicular to the longitudinal axis of the building, the interior columns are 50.8×50.8 cm on the ground floor and 45.72×45.72 cm on the remaining floors. The typical depth of the spandrel beams is 57.2 cm except for those on the second floor which have a depth of 76.2 cm. The floor system is RC flat slab, 25.4 cm thick at the second floor, 21.6 cm thick at the third to seventh floors and 20.3 cm thick at the roof. The story height seen as Fig. 4.1c. The foundation system (Fig. 4.1b) consists of

96.52 cm deep pile caps, supported by groups of two to four poured-in-place 50.8 cm diameter RC friction piles. These are centered under the main building columns. All the pile caps are connected by a grid of beams and each pile is roughly 12.2 m long. The building is situated on recent alluvium. The soil-boring log (Fig. 4.1d) shows that the underlying soil consists primarily of fine sandy silts and silty fine sands. Because the soil boring data only contains 45 feet depth soil data below the ground surface, the soil data below 45 feet are calculated by empirical formula. Zhou Xiyuan have completed statistical analysis of relationship between shear wave velocity and depth of soil for many cities in china. By comparing 45 feet depth soil data, the relationship between shear wave velocity and depth of soil for selected site is consistent with city Qinghuangdao of chain: $V_s = 143.9H^{0.371}$. The soil calculation depth is 200 m and the maximum shear wave velocity is 580.3m/s in this paper.



(a) typical floor plan

(b) foundation plan

(c) typical transverse section(N-S)

(d) soil boring data

Figure 4.1. Schematic representation and dimension of the structure

Table 4.1. Physical and mechanical parameters of structure members

	Location	Compressive strength (N/m ²)	Modulus of elasticity(N/m ²)	Density (kg/m ³)
Concrete	Columns, 1 st floor	3.45×10 ⁷	2.9×10 ¹⁰	2400
	Beams, columns and slabs, 2 nd floor	2.76×10 ⁷	2.55×10 ¹⁰	2400
	All other concrete 3 rd floor to roof	2.69×10 ⁷	2.28×10 ¹⁰	2400
Steel bar	Beams and slabs	2.76×10 ⁸	2.0×10 ¹¹	7800
	Columns	4.14×10 ⁸	2.0×10 ¹¹	7800

The SSI finite element model of E-W direction is shown in Fig. 4.2. In the model, plane strain element is used to simulate the soils and pile caps, beam element is used to simulate the beams, columns and piles, the contact interface between pile and soil is simulated by node-node contact element. Selecting bedrock accelerations data as the excitation, the seismic response of SSI is calculated and compared with the recorded data. The marginal spectrums of acceleration response are shown in Fig. 4.3 and Fig. 4.4, Fig. 4.5 to Fig. 4.7 respectively show the acceleration amplification factor, displacement envelope and story drift envelope of structural seismic response. Comparing the calculated data with the recorded data, the maximum relative errors are shown in Tab. 4.2.

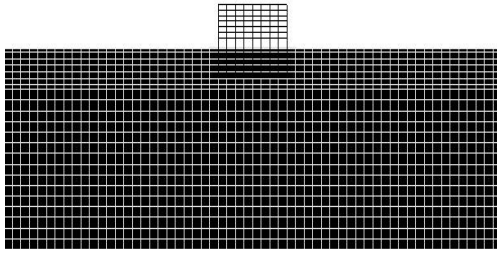
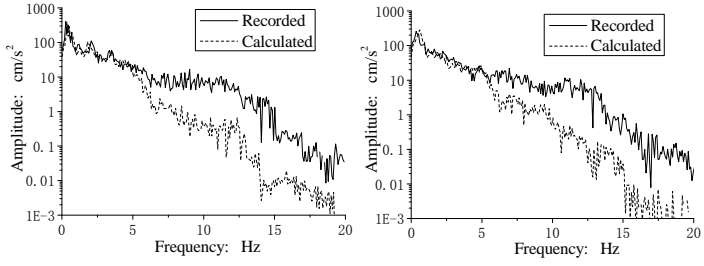
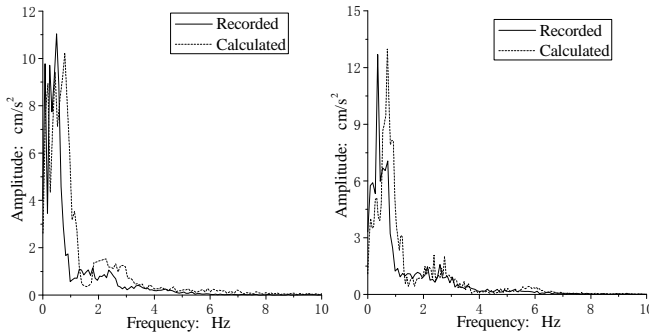


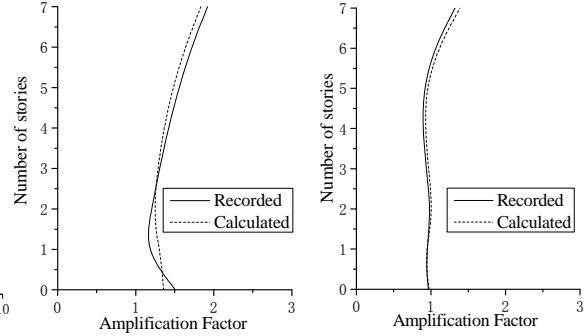
Figure 4.2. E-W direction finite element model of SSI



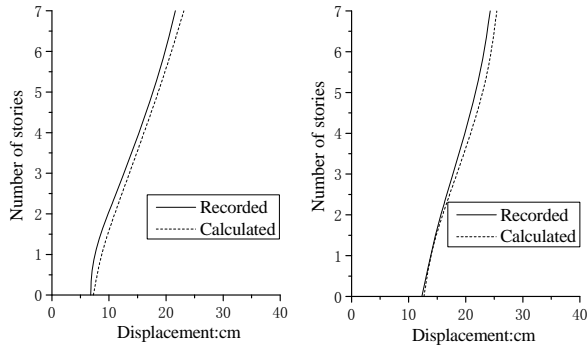
(a) E-W direction (b) N-S direction
Figure 4.3. Recorded and calculated marginal spectrum of ground motion



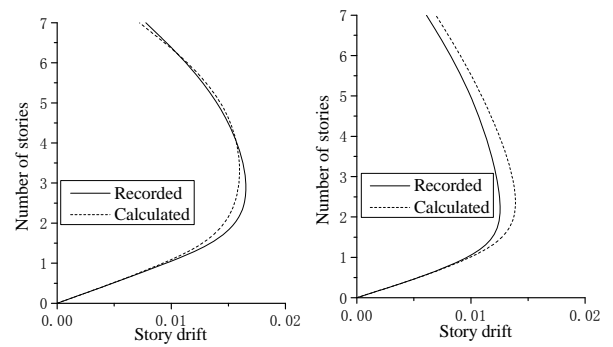
(a) E-W direction (b) N-S direction
Figure 4.4. Recorded and calculated marginal spectrum of roof motion



(a) E-W direction (b) N-S direction
Figure 4.5. Amplification factor of acceleration response



(a) E-W direction (b) N-S direction
Figure 4.6. The displacement envelope diagram



(a) E-W direction (b) N-S direction
Figure 4.7. Story drift envelope diagram

Table 4.2. The maximum errors of numerical simulation results

	Maximum acceleration (%)		Maximum displacement(%)		Story drift (%)	
	E-W	N-S	E-W	N-S	E-W	N-S
Foundation	9.89	0.98	7.04	3.22	—	—
2 nd floor	9.91	1.19	12.54	0.52	0.21	0.42
3 rd floor	0.59	3.2	10.72	2.11	8.77	13.68
6 th floor	5.62	3.98	3.91	6.49	6.38	8.22
Roof	4.5	5.02	6.84	4.66	7.23	13.56

It can be shown from above figures and table, the results of numerical simulation are very close to the recorded data. Comparing the marginal spectrum of ground motion, calculated results are almost same to the recorded data below 5Hz, and above 5Hz, the former is slightly lower than the latter. The reason is that equivalent linearization method ignores the high-frequency components of response.

Especially when the site is softer and the excitation is stronger, the error will be bigger. The above results are consistent with existing lessons learnt, such as Yoshida, Kausel, Youssef etc.

Comparing calculated acceleration marginal spectrum of structural roof motion with the recorded data, it can be seen that the structural natural frequency of numerical simulation result is obviously bigger than the recorded data in both east-west direction and north-south direction. It is shown that the structure was damaged, stiffness reduced and nature frequency decreased in previous earthquake. The problems of structural damage and material parameter variation due to earthquakes need to do further research in the subsequent numerical simulation.

It can be shown from Fig. 4.5 to Fig. 4.7 that the structural maximum acceleration, maximum displacement and story drift of calculated results are basically identical with the recorded data, but there are few errors larger than 10%, the detail results are given in Tab. 4.2.

5. CONCLUSION

Selecting the strong motion records from bedrock site, ground site and a 7-story RC structural site of western U.S. in 1994 Northridge earthquake, the time-frequency characteristics are analyzed by HHT method and numerical simulation of SSI system seismic response is studied in this paper. The results show that:

(1) Deep soft soil has significant filtering effect for frequency characteristics of ground motion, the low frequency components is amplified and the high frequency component is reduced, the predominant period has a tendency moving towards to long-period.

(2) The marginal spectrum distributions of structural foundation motion and roof motion are quite different, and the maximum amplitude of the latter is about 4 times of the former. The acceleration of roof motion has considerable amplification.

(3) The structural natural frequency of numerical simulation result is obviously bigger than the recorded data in both east-west direction and north-south direction. In the process of numerical simulation, it should be given sufficient attention to the structural damage and material parameter variation due to earthquakes.

(4) The structural maximum acceleration, maximum displacement and story drift of numerical simulation results are basically identical with the recorded data, besides few larger errors. The results show that the numerical model built in this work has high accuracy.

ACKNOWLEDGEMENT

This research described herein was supported by National Natural Science Foundation of China through Grant Number: 50978198; 90915011. The authors gratefully acknowledge this support. All computation was done at the State Key Laboratory of Disaster Reduction in Civil Engineering, Tongji University, Shanghai, China. The authors thank Dr Li Yincheng, Dr Zhang Ting, Dr Zhang Wei, Dr Yuan Weize and other reviewers for providing insightful comments that greatly enhanced this paper. All opinions expressed in this paper are solely those of the authors.

REFERENCES

- Yang J N, Lei Y, Pan s, et al.(2003). System identification of linear structures based on Hilbert-Huang spectral analysis. Part 1: Normal modes. *Earthquake Engineering and Structural Dynamics*.**32:9**,1443-1467.
- Yang J N, Lei Y, Pan s, et al.(2003). System identification of linear structures based on Hilbert-Huang spectral analysis. Part 2: Complex modes. *Earthquake Engineering and Structural Dynamics*.**32:10**,1533-1554.
- Chen Q J, LI Y C, Hu C Y. (2010). Study on energy distribution of special long-period ground motion based on

- orthogonal Hilbert-Huang transform method. *Chinese Quarterly of Mechanics*. **31:4**,548-554.
- Lou M L, Wu J N. (1999). Seismic Response analysis of pile foundation structure system. *Chinese Civil Engineering Journal*. **32:5**,56-61.
- Wang F X, He Z, Ou J P.(2003). The elastic seismic response analysis of pile-soil-structure interaction system. *World Earthquake Engineering*. **19:2**,58-66.
- Chen Q J, Jiang w h, Lou M L.(2003). Analysis of three-dimensional nonlinear seismic response of pile group foundation. *Journal of Vibration and Shock*. **22:3**,98-102.
- Ainir M, Kaynia, Eduardo Kausel.(1991). Dynamics of piles and pile groups in layered soil media. *Soil Dynamic and Earthquake Engineering*. **10:8**,386-401.
- Gong M S, Xie L L.(2003). Discussion on the application of HHT method to earthquake engineering. *World Earthquake Engineering*. **19:3**,39-43.
- Huang N E, et al.(1998). The empirical mode decomposition and Hilbert spectrum for nonlinear and non-stationary time series analysis. *Proceedings of The Royal Society of London*. **454(1971)**:903-906.
- Huang N E.(2001). HHT: a review of the methods and many applications for nonsteady and nonlinear data analysis. Laboratory for Hydrospheric Processes, NASA Goddard Flight Center, Greenbelt, MD.
- Martin P P, Seed H B.(1982). One-dimensional dynamic ground response analyses. *Journal of the Geotechnical Engineering Division*.**108:7**,935-952.
- Hadjian A H, Tseng W S, Luo D.(1993). The Learning from the large scale lotung soil-structure interaction experiments(I). *World Earthquake Engineering*. **9:3**,41-52.
- Seed H B, Idriss I M.(1970). Soil moduli and damping factors for dynamic response analyses. Report No. EERC 70-10, Earthquake Engineering Research Center, University of California, Berkeley.
- Sun J I, Colesorkhi R, Seed H B.(1988). Dynamic moduli and damping ratios for cohesive soils. Report No. EERC88/15, Earthquake Engineering Research Center, University of California, Berkeley.
- Idriss I M, Sum J I.(1992). SHAKE91: A computer program for conducting equivalent linear seismic response analyses of horizontally layered soil deposits. User's Guide, University of California, Davis, California.
- Vucetic M, Dobry R.(1991). Effect of soil plasticity on cyclic response. *Journal of Geotechnical Engineering*. **117:1**,89-107.
- Ishibashi I, Zhang X.(1993). Unified dynamic shear moduli and damping ratios of sand and clay. *Soils and Foundations*.**33:1**,182-191.
- M.I. Todorovska, S.S. Ivanovic', M.D. Trifunac.(2001). Wave propagation in a seven-story reinforced concrete building: I. Theoretical models. *Soil Dynamics and Earthquake Engineering*. **21:3**,211-223.
- M.I. Todorovska, S.S. Ivanovic', M.D. Trifunac.(2001). Wave propagation in a seven-story reinforced concrete building: II. Observed wavenumbers. *Soil Dynamics and Earthquake Engineering*. **21:3**,225-236.
- M.D. Trifunac, S.S. Ivanovic', M.I. Todorovska.(2003). Wave propagation in a seven-story reinforced concrete building: III. Damage detection via changes in wavenumbers. *Soil Dynamics and Earthquake Engineering*.**23:1**,65-75.
- S.S. Ivanovic', M.D. Trifunac, E.I. Novikova et al.(2000). Ambient vibration tests of a seven-story reinforced concrete building in Van Nuys, California, damaged by the 1994 Northridge earthquake. *Soil Dynamics and Earthquake Engineering*. **19:6**,391-411.
- Zhou X Y, Wang G J, Su J Y.(1990). Site·Foundation·Design earthquake, Beijing, Earthquake Press.China.
- Yoshida N, Kobayashi S, Suetomi I.(2002). Equivalent linear method considering frequency dependent characteristics of stiffness and damping. *Soil Dynamic and Earthquake Engineering*. **22:3**,205-222.
- Kausel E, Assimaki D.(2002). Seismic simulation of inelastic soil via frequency-dependent moduli and damping. *Journal of Engineering Mechanics*. **128:1**,34-46.
- Youssef M A, Hashash D P.(2001). Non-linear one-dimensional seismic ground motion propagation in the Mississippi embayment. *Engineering Geology*.**62:2**,185-206.